

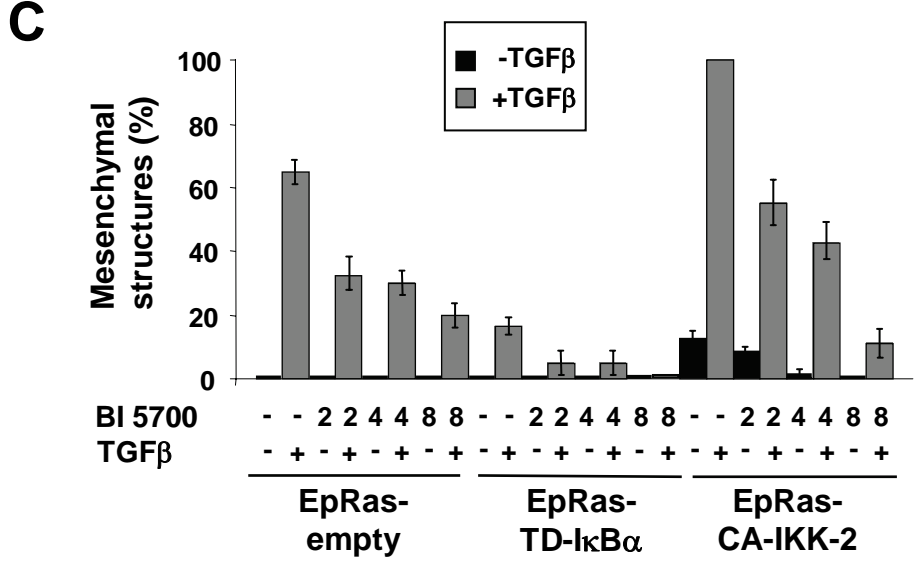
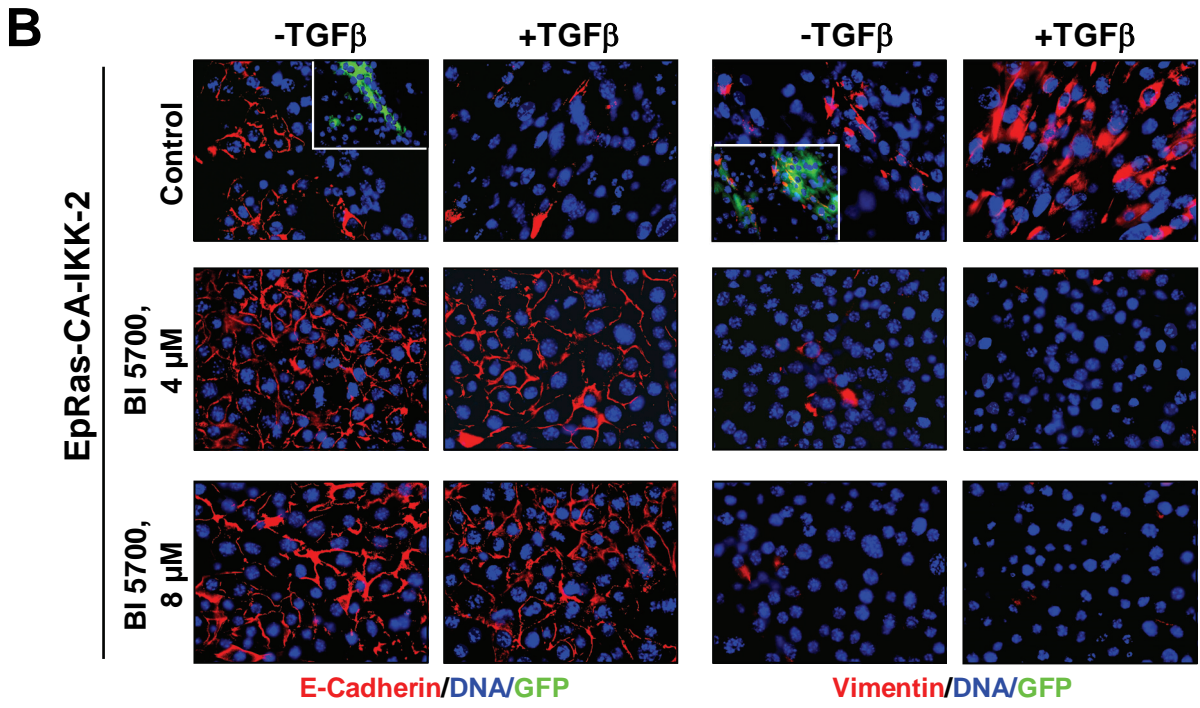
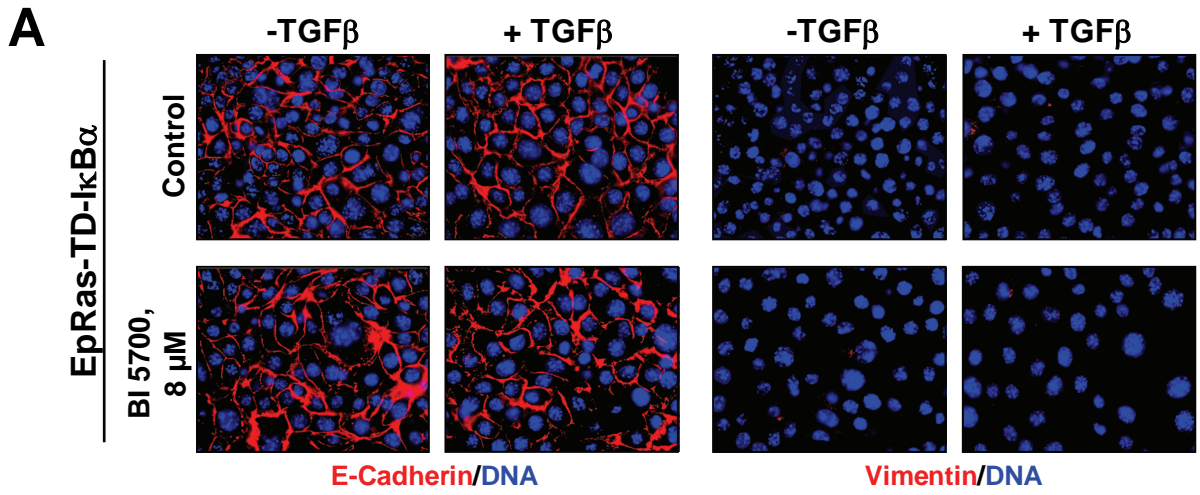
Supplementary Figure Legends

Supplementary Figure S1. The IKK2 inhibitor blocks EMT caused by IKK2-specific NFκB pathway activation. EpRas cells prevented from or induced to undergo EMT by TD-IκBα (A) or CA-IKK2 (B) were cultivated on porous supports in the presence (+) or absence (-) of TGFβ (5 ng/ml; days 2-7) and treated or not treated (control) with BI 5700 at the concentrations indicated. Cells were then immunostained for E-cadherin or Vimentin (red) as indicated, with DAPI counterstaining for DNA (blue). E-cadherin-negative/Vimentin-positive cells strongly expressing the CA-IKK2 transgene (insets in control – and + TGFβ panels) are indicated by GFP expression (green, see insets). Original magnification, x400. (C) Quantification of cells in mesenchymal structures as the percentage from >300 randomly chosen cells per filter in the presence or absence of TGFβ (light versus dark bars, respectively). At the indicated concentrations (in μM), the IKK2 inhibitor BI 5700 dose-dependently blocked EMT induced by either IKK2 or TGFβ.

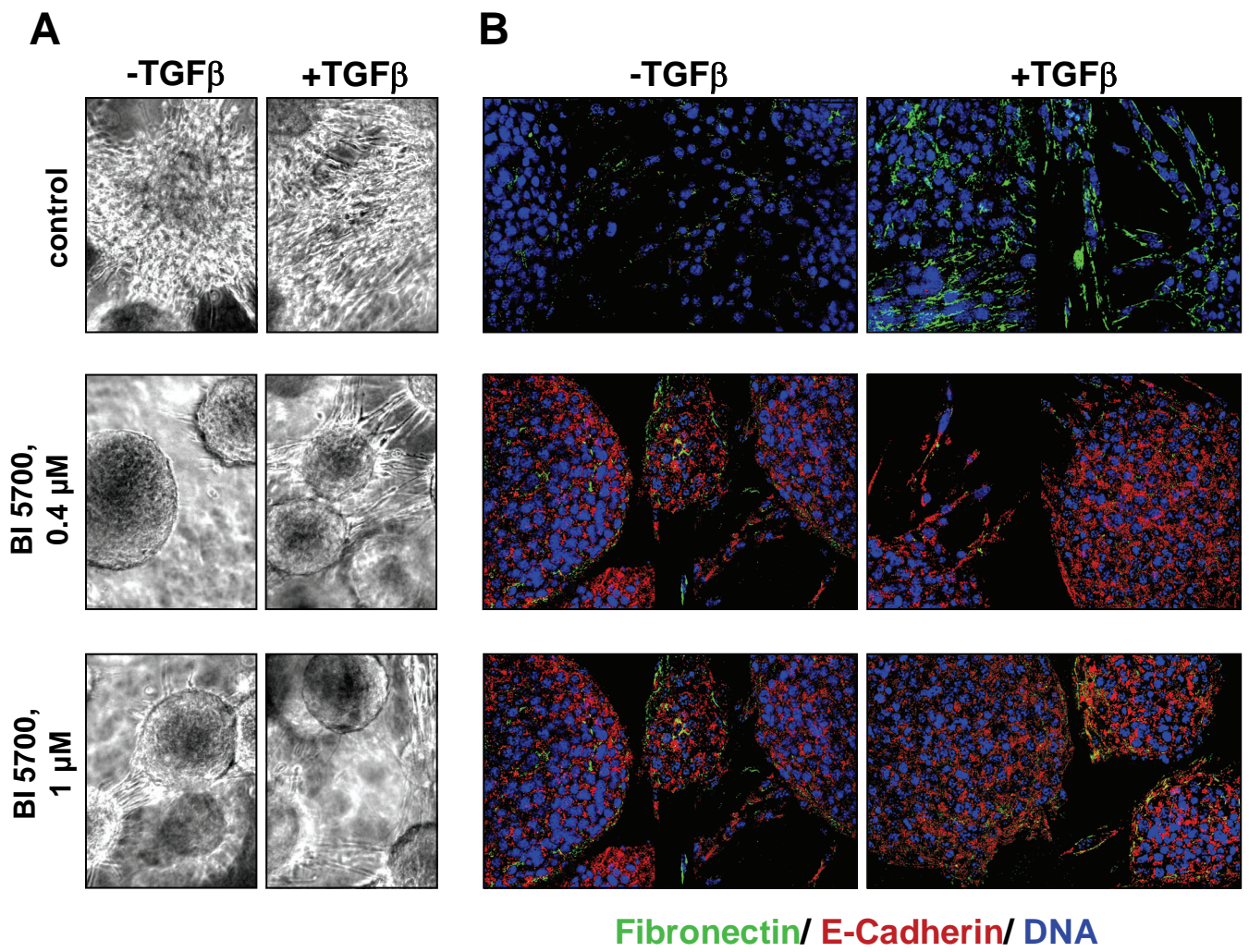
Supplemental Figure S2. Inhibition of IKK2 causes reversal of constitutive EMT in mesenchymal colon carcinoma cells (CT26). CT26 cells were seeded into collagen gels and allowed to form structures for 2 days. BI 5700 was added or not added at day 2 at the concentrations indicated. At day 3, gels were treated (+) or not treated (-) with 5 ng/ml TGFβ for 6 further days. (A). Bright field photographs of the unordered clumps of untreated fibroblastoid cells and the compact cell balls formed by BI 5700-treated cells plus or minus TGFβ. (B). Confocal micrographs of cell structures from the gels depicted in (A) are shown. Untreated cells plus TGFβ show the expected, complete EMT-phenotype (high fibronectin, no E-cadherin; (25), while BI 5700-treated cells reverted to a epitheloid phenotype unaffected by TGFβ (no or little fibronectin, upregulation of cytoplasmic E-cadherin, comparable to effects obtained with TGFβRII-inhibitor treatment; Ref. 25).

Supplementary Figure S3. Pharmacokinetic analysis of BI 5700. Time course of BI 5700 plasma concentration in mice after a single p.o. dose of 150 mg/kg (n=3).

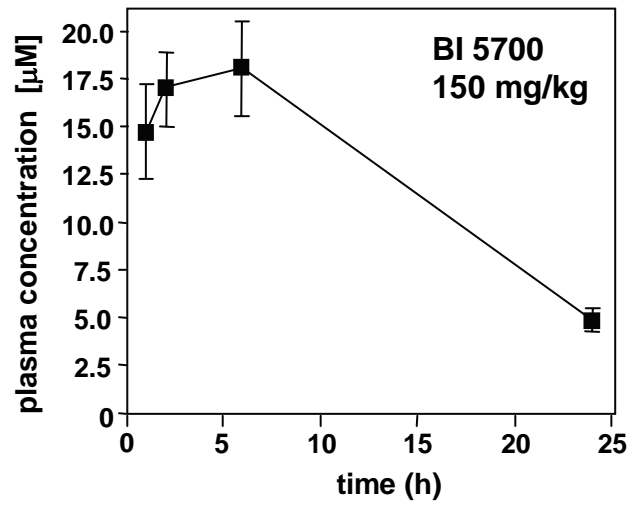
Supplementary Figure S4. Evaluation of metastases upon treatment with BI 5700. (A) In the experimental set-up described in Figure 5, 14-15 serial sections (0.3 mm apart) through the lungs of control- and BI 5700-treated mice were evaluated by counting metastases in the sections grouped into 4 different size classes (top, see Materials and Methods). Numbers of small metastases showed no significant differences, but 2-3 fold fewer metastases of the two large size classes were observed in the BI 5700-treated mice. Significant differences revealed by Student's t-test are shown as P-values; NS= not significant. (B) Histological sections stained with H&E and photographed at low and high magnification (insets, red frame) are shown. 2-4 areas from the lungs of different animals have been mounted in the panels shown, to display the variability of metastatic sizes and histological appearance obtained. Dotted, black lines; outlines of typical metastases seen in control- and BI 5700-treated lungs.



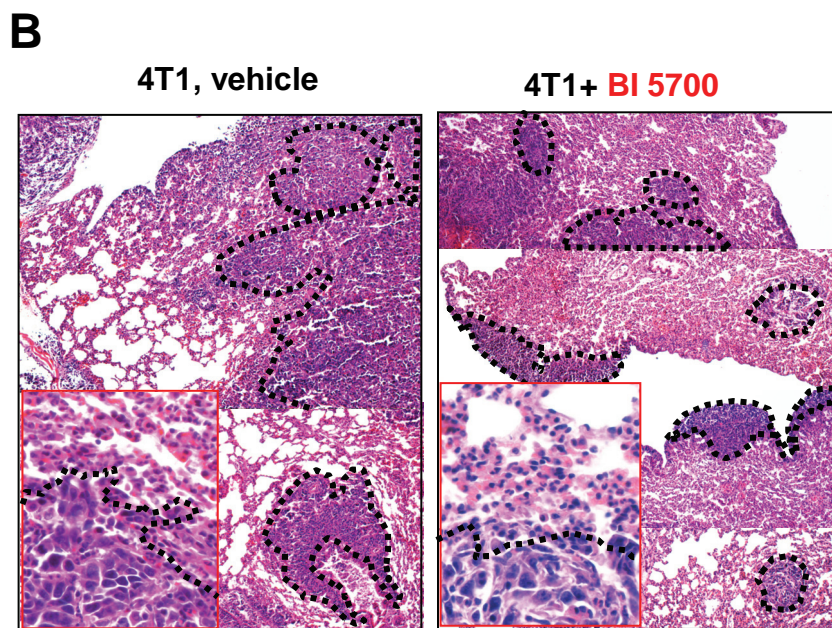
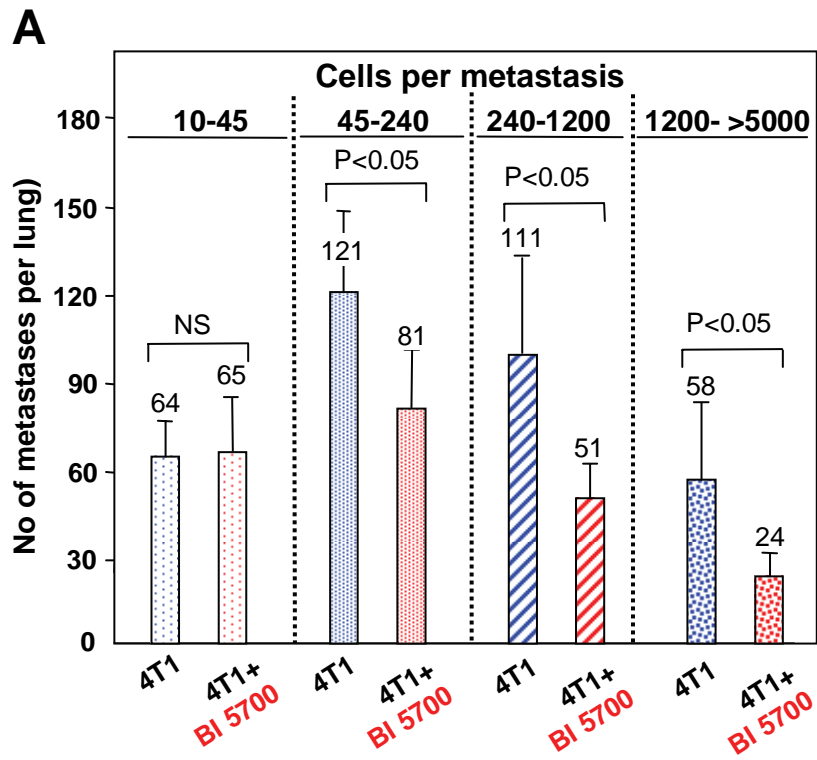
Supplementary Fig. S1, Huber et al.



Supplementary Fig. S2, Huber et al.



Supplementary Fig. S3, Huber et al.



Supplementary Fig. S4, Huber et al.